



# Using primary murine intestinal enteroids to study dietary TAG absorption, lipoprotein synthesis, and the role of apoC-III in the intestine<sup>S</sup>

Javeed Jattan,\* Cayla Rodia,\* Diana Li,\* Adama Diakhate,\* Hongli Dong,\* Amy Bataille,\* Noah F. Shroyer,<sup>†</sup> and Alison B. Kohan<sup>1,\*</sup>

Department of Nutritional Sciences\*, University of Connecticut, Storrs, CT; and Department of Medicine Section of Gastroenterology and Hepatology,<sup>†</sup> Baylor College of Medicine, Houston, TX

**Abstract** Since its initial report in 2009, the intestinal enteroid culture system has been a powerful tool used to study stem cell biology and development in the gastrointestinal tract. However, a major question is whether enteroids retain intestinal function and physiology. There have been significant contributions describing ion transport physiology of human intestinal organoid cultures, as well as physiology of gastric organoids, but critical studies on dietary fat absorption and chylomicron synthesis in primary intestinal enteroids have not been undertaken. Here we report that primary murine enteroid cultures recapitulate *in vivo* intestinal lipoprotein synthesis and secretion, and reflect key aspects of the physiology of intact intestine in regard to dietary fat absorption. We also show that enteroids can be used to elucidate intestinal mechanisms behind CVD risk factors, including tissue-specific apolipoprotein functions. Using enteroids, we show that intestinal apoC-III overexpression results in the secretion of smaller, less dense chylomicron particles along with reduced triacylglycerol secretion from the intestine. **■** This model significantly expands our ability to test how specific genes or genetic polymorphisms function in dietary fat absorption and the precise intestinal mechanisms that are critical in the etiology of metabolic disease.—Jattan, J., C. Rodia, D. Li, A. Diakhate, H. Dong, A. Bataille, N. F. Shroyer, and A. B. Kohan. Using primary murine intestinal enteroids to study dietary TAG absorption, lipoprotein synthesis, and the role of apoC-III in the intestine. *J. Lipid Res.* 2017. 58: 853–865.

**Supplementary key words** intestinal lipid transport • chylomicrons • stem cells • organoids • dietary fat absorption • apolipoprotein C-III • triglyceride

The intestine plays a crucial role in regulating whole-body lipid homeostasis through dietary fat absorption and secretion, and through its endocrine secretions of incretin hormones and immune mediators. The intestine synthesizes a specialized lipoprotein, the chylomicron, which contains both dietary triglyceride (TAG) and cholesterol, in addition to both structural and functional apolipoprotein cargo. apoB-48 provides structure to the nascent chylomicron, while apoA-IV, apoA-I, and apoC-III function in the periphery to modify plasma lipid metabolism and clearance, interact with inflammatory apparatus for efficient clearance of dietary lipopoly-saccharide and oxidized lipids, and modulate insulin signaling and glucose metabolism (1–3). Therefore, the intestine and its secreted chylomicron are critical regulators of metabolic disease.

Despite the importance of the intestine in raising plasma TAG levels in the postprandial state and in apolipoprotein secretion, mechanistic studies are difficult to carry out. This is due to a lack of suitable *ex vivo* cell culture models that are nontransformed yet stable enough in culture for extended studies and genetic manipulations. The intestine is difficult to model *ex vivo* because enterocytes are in constant turnover, and are only replenished by intestinal stem cells (ISCs), which in native tissue reside at the bottom of the crypt-villus axis (4). ISCs give rise to all intestinal epithelial cells, including enterocytes, enteroendocrine cells, goblet

Abbreviations: ALPI, enterocyte-specific alkaline phosphatase; DGAT, acyl-CoA:diacylglycerol acyltransferase; DPBS, Dulbecco's PBS; hu-apoC-III Tg, human apoC-III transgenic; ISC, intestinal stem cell; KLF4, Krüppel-like factor 4; KRT, cytokeratin; LGR5, leucine-rich repeat-containing G protein-coupled receptor 5; MAG, monoacylglycerol; MGAT2, acyl-CoA:monoacylglycerol acyltransferase 2; MTTP, microsomal triglyceride transfer protein; OA, oleic acid; PC, phosphatidylcholine; TAG, triacylglycerol (triglyceride); TEM, transmission electron microscopy; TFF3, trefoil factor 3; SI, sucrase-isomaltase; VIL1, brush border villin.

<sup>1</sup>To whom correspondence should be addressed.

e-mail: alison.kohan@uconn.edu

**S** The online version of this article (available at <http://www.jlr.org>) contains a supplement.

This work was supported by National Institute of Diabetes and Digestive and Kidney Diseases Grant DK101663 and USDA National Institute of Food and Agriculture Grants 11874590 and 2015-31200-06009 (Hatch Formula Funds) (all to A.B.K.). The content is solely the responsibility of the authors and does not necessarily represent the official views of the National Institutes of Health. The authors have no conflicts of interest to report.

Manuscript received 9 August 2016 and in revised form 18 January 2017.

Published, JLR Papers in Press, February 3, 2017

DOI <https://doi.org/10.1194/jlr.M071340>

Copyright © 2017 by the American Society for Biochemistry and Molecular Biology, Inc.

This article is available online at <http://www.jlr.org>

cells, tuft cells, and Paneth cells (5, 6). In an ex vivo system, those enterocytes cannot be replenished unless they are genetically transformed or come from a cancer model in which normal metabolic and apoptotic pathways are dysregulated, as in Caco-2 cells. Primary mouse enteroids, originally established by Sato and Clevers in 2009, avoid these drawbacks (7). In this stem cell culture system, isolated intestinal crypts containing ISCs expand in culture to form organoid structures, which retain in vivo intestine-specific characteristics, including the proliferation and maintenance of all absorptive and secretory cell lineages from ISC precursors.

The enterocyte is the functional unit of dietary lipid absorption, chylomicron synthesis, and secretion. The enterocyte takes up FFAs and monoacylglycerol (MAG), which are generated in the intestinal lumen by pancreatic lipase hydrolysis of dietary TAG. The enterocyte resynthesizes TAG from the FFA and MAG dietary substrates through the 2-MAG pathway, catalyzed by acyl-CoA:monoacylglycerol acyltransferase 2 (MGAT2) and acyl-CoA:diacylglycerol acyltransferase (DGAT)1 activity in the endoplasmic reticulum lumen (3). On the endoplasmic reticulum membrane, microsomal TAG-transfer protein (MTTP) lipidates apoB-48 (and also apoB-100 in mice), which is required for mature chylomicron formation. This prechylomicron contains TAG and cholesterol in its core and phospholipids on its exterior (4). As the prechylomicron matures, it obtains its apolipoprotein cargo, including apoA-I, apoC-III, and apoA-IV. It is the constellation of these apolipoproteins on the chylomicron that will later direct the metabolism of the particle in the blood and by peripheral tissues such as adipose and liver (1).

apoC-III is an exchangeable lipoprotein produced by both the liver and intestine, and found on both chylomicrons and VLDLs. The plasma concentration of apoC-III is elevated in type 1 diabetics, and is an independent predictor of CVD (8, 9). In plasma, apoC-III resides on both TAG-rich lipoproteins and HDLs. Overproduction of apoC-III and TAG-rich lipoproteins is a common feature in patients with hypertriglyceridemia (10, 11). apoC-III also stimulates hepatic synthesis and secretion of VLDLs (12, 13). We have reported that mice overexpressing apoC-III have a delayed rate of lipid absorption and secretion into lymph (14). Though significant progress has been made in understanding the mechanisms that govern these plasma and hepatic effects of apoC-III, much less is known about the function of apoC-III in the intestinal lipoprotein synthesis pathway and its potential effect on the metabolism of dietary lipid and subsequent impact on CVD risk. This is an important gap in our knowledge because the intestinal lipoprotein synthesis and secretion pathway is unique from the liver VLDL pathway (15).

In order to ask mechanistic questions on the role of apoC-III in the intestinal chylomicron synthesis pathway, we first had to adapt the primary enteroid model. Our data is the first to show that primary murine enteroids are a viable model to recapitulate intestinal fat absorption by taking up [<sup>3</sup>H]FFA and secreting [<sup>3</sup>H]TAG along with apoB-48 and other apolipoproteins, as well as a

chylomicron-sized particle. In addition, enteroids can be used to measure critical mechanisms surrounding dietary fat absorption, including the role of apoC-III on intestinal fat absorption.

## MATERIALS AND METHODS

### Animals

C57BL/6J or human apoC-III transgenic (hu-apoC-III Tg) mice [generously provided by Dr. H. Dong, University of Pittsburgh, and originally generated by Dr. Jan Breslow (14, 16)] aged 8–12 weeks were used for the isolation of primary intestinal crypts. Hu-apoC-III Tg mice overexpress human apoC-III (at approximately five times normal murine apoC-III levels) and have fasting plasma TAG levels of 500–700 mg/dl. Hu-apoC-III Tg mice are homozygous for the transgene, which retains the human apoC-III promoter to drive expression in the same tissue distribution pattern as the endogenous mouse apoC-III. Transgenic mice express both murine and human apoC-III, but have no compensatory changes in endogenous mouse apoC-III expression (14). In our colony, hu-apoC-III Tg mice have been extensively backcrossed to C57BL/6J mice, therefore we used our own colony of transgenic and C57BL/6J (WT) mice throughout these studies. Mice were housed (three to four per cage) in a temperature-controlled (21 ± 1°C) vivarium on a 12 h light-dark cycle. All animals received free access to water and chow diet (LM-485 mouse/rat sterilizable diet; Harlan Laboratories). All animal procedures were performed in accordance with the University of Connecticut Internal Animal Care and Use Committee and in compliance with the National Institutes of Health Guide for the Care and Use of Laboratory Animals.

### Isolation of crypts and primary culture

ISCs were isolated according to the procedure of Sato et al. (7) with minor modifications (17). Animals were euthanized via CO<sub>2</sub> inhalation and the intestine removed, with care to avoid the first 3 cm immediately proximal to the stomach where Brunner's glands reside. The intestine was rinsed and washed twice in ice-cold Dulbecco's PBS (DPBS). The tissue was then divided in three equal segments: the first third was duodenum; the second third was jejunum; and the third was ileum. These tissues were kept in ice-cold DPBS for 2 h at 4°C. The tissue was then cut longitudinally and minced. The minced tissue was then placed in chelation buffer (DPBS without Ca<sup>2+</sup> and Mg<sup>2+</sup>, with 2 mM EDTA) in a 15 ml tube on a rocker for 30 min at 4°C. The tissue was allowed to settle and then the chelation buffer was removed and replaced with 5 ml of dissociation buffer (43.4 mM sucrose, 54.9 mM D-sorbitol in DPBS) and shaken by hand for 3 min to dissociate individual crypts from whole tissue. After viewing an aliquot under 20× magnification to determine adequate crypt dissociation from villus tips (which are the first to break free of the mucosal layer), the crypt/dissociation buffer mixture was filtered through a 70 μm nylon mesh cell strainer (Fisher; catalog number 22363548). The crypts were centrifuged at 150 *g* for 10 min and the supernatant was removed and then washed twice in 5 ml of DPBS. Finally, the crypt pellet was resuspended at a concentration of 400 crypts/50 μl of depolymerized Matrigel (BD Biosciences, Franklin Lakes, NJ) containing 1 μl of R-spondin 1 (250 μg/ml), 1 μl of Noggin (50 μg/ml), and 0.25 μl of EGF (100 μg/ml). The Matrigel/crypt suspension was plated in 24-well plates at a density of 50 μl/well and allowed to polymerize at 37°C in a 5% CO<sub>2</sub> incubator. Five hundred microliters of enteroid medium [Advanced DMEM/F12 (12634-010; Life Technologies, Carlsbad, CA) with 2 mM L-glutamine, 10 mM HEPES, 100 U/ml penicillin/100 μg/ml streptomycin, and

1× N2 and 1× B27 supplements] were then added to the wells. Fresh enteroid growth medium was replaced the following morning with complete growth medium containing the enteroid medium plus 1 µl of R-spondin 1 (250 µg/ml), 1 µl of Noggin (50 µg/ml), and 0.25 µl of EGF (100 µg/ml). Medium was replaced every 3–4 days with complete enteroid growth medium, except where indicated.

### Enteroid culture and differentiation

Primary crypts were propagated in culture as described in Fig. 1, with minor modifications (7, 18). When enteroids formed 3D hollow balls, which we call mature enteroids, they were either used for lipoprotein experiments or passed. Enteroids were passaged by removing medium, washing three times with ice-cold DPBS, and then washing by spinning at 150 *g* for 5 min in a conical tube. Enteroids were gently broken open by repeated pipetting (5–20 times) with a P200 Pipetman (Gilson, Middleton, WI). Enteroids were passaged by breaking the mature enteroids into individual crypts, which reform mature enteroids in approximately 7–10 days, or, alternatively, enteroids were broken open into multicrypt pieces, which form mature enteroids in approximately 4 days. Regardless of the density of passage, the crypts were placed back into Matrigel with complete growth medium as described above. Enteroid cultures were propagated from three to six different C57Bl/6J WT mice and at least three to six different hu-apoC-III Tg mice (yielding *n* = 3–6 unique enteroid strains).

Experiments were conducted using different enteroid strains, enteroids at different passage numbers, and multiple experimental days. We maintained enteroids in culture for at least 20 passages. Differentiated enteroids were cultured by passaging mature enteroids using a p1000 pipette and resuspending them in Matrigel without R-spondin for 4 days. To directly compare enteroid lines to each other, we counted crypts and plated the same number of crypts at day 1, adhering to identical culture conditions throughout the experiment, and isolation on day 10.

### Treatment with FA

Though mature enteroids mimic the 3D architecture of the intestine, they do not contain pancreatic lipase, which is necessary to hydrolyze TAG to FFA and MAG. To mimic dietary fat absorption, one approach we used was to treat with BSA-bound FFA. Oleic acid (OA) (Nu-Check Prep) was prepared as 4 mM stock solutions in complex with FA-free BSA at a 1:4 molar ratio and the stock contained butylated-hydroxytoluene 0.1% (19). Enteroids not receiving the 400 µM OA:BSA complex were treated with an equivalent amount of BSA. Mature enteroids were dissociated from Matrigel by washing with ice-cold DPBS, followed by a 150 *g* spin for 10 min. After removing the supernatant, the intact enteroids were then placed in 1 ml of treatment medium in a 1.5 ml Eppendorf tube containing 0.5 µCi of radiolabeled OA (American Radiolabeled Chemicals), 1:1,000 Y27623 Rho-kinase inhibitor compound (Sigma), 400 µM OA:BSA or BSA alone, and enteroid growth medium. The enteroids were very gently opened by pipetting up and down with a p1000 pipette, followed by incubation with the lids open in a 37° 5% CO<sub>2</sub> incubator for 2 h. After 2 h, the enteroids were centrifuged at 150 *g* for 10 min and the supernatant collected. Following an additional wash and centrifuge with 1 ml of DPBS (which was added to the medium samples), the enteroids were resuspended in 1 ml of enteroid growth medium and placed back in the incubator for 4–6 h with the lid to their tubes left open for gas exchange. The medium and cell pellet were then collected via centrifugation at 150 *g* for 10 min. For experiments with radiolabeled-FFA, we used 0.5 µCi of OA [9-10-3H(N)] spiked into the OA:BSA mix or 0.5 µCi cholesterol [4-14C] (American Radiolabeled Chemicals, Inc., St. Louis, MO; catalog numbers ART 0198 and ARC 0857, respectively).

### Caco-2 cell culture

Caco-2 cells were obtained from American Type Culture Collection (Manassas, VA) and grown at 37°C with 5% CO<sub>2</sub> in growth medium (DMEM with 10% FBS). For propagation, cells were split (1:6) when they reached 75% confluence. Medium was changed every other day. For TAG secretion studies, cells were maintained until they reached confluence and then given fresh medium for an additional 17 days post confluence. As described in by Nauli et al. (20), this protocol produces the most abundant chylomicron-like apoB-lipoproteins. For direct comparisons between enteroids and Caco-2 cells, we isolated genomic DNA from the parallel cultures of Caco-2 cells and enteroids at the conclusion of each experiment, and normalized measurements to total genomic DNA concentrations in the enteroids and Caco-2 cells.

### Preparation of lipid micelles

Stock solutions of OA, phosphatidylcholine (PC), 2-palmitoylglycerol, and cholesterol were prepared in chloroform. Stock solutions of sodium taurocholate were prepared in PBS. To prepare lipid micelles, OA, PC, 2-palmitoylglycerol, and cholesterol were combined into a glass vial and dried under a stream of nitrogen. After the lipids were completely dried, warm sodium taurocholate was added to the mixture and vortexed. The mixture was brought to final concentration with warm PBS. The final lipid micelle preparation, therefore, consisted of PBS containing 6 mM OA, 20 mM TC, 2 mM 2-palmitoylglycerol, 0.5 mM cholesterol, and 2 mM PC. Micelles were diluted prior to being vortexed with 0.5 µCi of [<sup>3</sup>H] OA or 0.5 µCi [<sup>14</sup>C]cholesterol to a final concentration in the treatment medium of 0.6 mM OA, 2 mM taurocholate, 0.2 mM 2-palmitoylglycerol, 0.05 mM cholesterol, and 0.2 mM PC. Lipid micelles were delivered to the medium of Caco-2 cells and the lumen of enteroids as with the treatment of FFA above. For treatment with BODIPY-C12 FFA (Molecular Probes, Inc., catalog number D3822), BODIPY-FFA was incorporated into mixed micelles with [<sup>3</sup>H]OA.

### Isolation of chylomicrons

To isolate chylomicrons, mature enteroids, at days 7–10 in culture, were treated with 400 µM OA, or BSA alone, to stimulate chylomicron secretion (as described above) for 2 h. After 2 h, the medium was replaced with fresh medium for 4 h and then it was pooled from three separate wells from a 12-well plate. The medium was immediately centrifuged at 43,000 *g* for 3 h at 4°C in a Beckman TLA 110 rotor (Beckman Instruments, Palo Alto, CA). The top 50 µl was isolated for transmission electron microscopy (TEM). Chylomicrons were used in assays within 24 h of isolation unless otherwise noted.

### TEM

Fresh chylomicron samples were stained with 2% phosphotungstic acid (pH 6.0) for 5 min on carbon film (CF400-CU; Electron Microscopy Sciences, Hatfield, PA), allowed to dry, and then examined with a transmission electron microscope (JEOL, Peabody, MA). Images were documented with an AMT Advantage Plus CD camera, as described previously (21). Lipoprotein particles were measured and counted using ImageJ software.

### Folch extraction of tissue lipids and thin-layer chromatography

After treatment with OA bound to BSA or OA micelles for 6 h, both medium and cells were isolated and added to 10 ml of chloroform/methanol (2:1, v/v) for Folch extraction, as described previously (22). The extracted lipids were then separated on silica gel 60 plates using a solvent system of petroleum ether/ethyl ether/glacial acetic acid with 25:5:1 vol ratio. After visualizing the



samples and the comigrating reference standards by staining with iodine vapor, samples were scraped into scintillation vials and left overnight in scintillation liquid to elute the radioactive lipid from the gel (OptiFluor for aqueous samples) for counting of radioactivity.

### Protein isolation and Western blot analysis

Cell lysates were prepared by collecting three wells of enteroids in 1× RIPA lysis buffer with 1× protease inhibitor (protease inhibitor cocktail; Thermo Fisher). Medium was added directly to 4× Laemmli buffer. The BCA protein assay kit (Pierce) was used to determine the protein concentration of the cell lysates, while medium samples were loaded by volume. The cell lysates (20–40 μg protein) were then separated by 7.5–12% SDS-PAGE and transferred to polyvinylidene difluoride membranes in a transfer buffer consisting of 20 mM Tris-HCl (pH 6.8), 154 mM glycine, and 20% methanol. Membranes were blocked with 5% nonfat dry milk in Tris-buffered saline with 0.1% Tween and incubated with species-appropriate primary antibodies overnight at 4°C: apoB 1:250 (Abcam; ab20737), apoA-IV 1:1,000 (Cell Signaling; 1D6B6), and apoA-I 1:2,000 (Abcam; ab52945). Secondary antibodies, goat-anti-mouse IgG-HRP1:2000 (SantaCruz Biotechnology, sc-2005) and anti-rabbit IgG-HRP 1:2000 (Sigma, A4914), were incubated for 1 h at room temperature. Membranes were incubated with Clarity Western ECL substrate (Bio-Rad) for 5 min before being imaged using ChemiDoc MP imaging system (Bio-Rad).

### Gene expression via RT-PCR

Total RNA was isolated from three wells per treatment using Tri-Reagent (Ambion) according to manufacturer's instructions. cDNA was synthesized using 2 μg of RNA. Expression of all mRNAs was determined by quantitative real-time PCR using CFX Connect real-time system (Bio-Rad) along with iQ™ SYBR® Green Supermix (Bio-Rad) according to the manufacturer's instructions. Sequences for primers are provided in supplemental Table S1. Expression of GAPDH was used as a control and the amount of each mRNA was calculated relative to this control. The relative amount of mRNA was calculated using the comparative threshold cycle method.

### Statistics

All data are presented as mean ± SEM. Statistics were performed using GraphPad Prism (version 6.0). The differences between the WT and hu-apoC-III Tg enteroids or between Caco-2 cells and enteroids were analyzed by Student's *t*-test. Analyses of more than one experimental group, compared with control tissue, were analyzed by one-way ANOVA using Graph Pad Prism 6.0. Differences were considered significant at  $P < 0.05$ .

## RESULTS

### Murine intestinal crypts differentiate into mature enteroids and express key machinery for dietary lipid absorption and secretion

We used a 3D culture system in which isolated crypts from murine intestine propagate in polymerized Matrigel to form mature enteroids composed of differentiated cells surrounding a central lumen (7). In this model, the apical surface of the enteroid is located within the enteroid sphere and the basolateral surface lies in contact with Matrigel and culture media. The stem cells in the crypts expanded and differentiated in response to the growth factors, EGF, R-spondin, and Noggin, resulting in mature enteroids with epithelial cells arranged around a central lumen filled with mucus, with new crypts decorating the basolateral surface after a 7–10 day culture (Fig. 1A), whereas Caco-2 cells (the most commonly used cell culture model of the intestine) grew as a 2D monolayer (Fig. 1B). A major advantage of the enteroid culture model is that it reflects the *in vivo* architecture of the intestine (with a luminal and basolateral surface). Though they are not transformed, enteroids can be passaged due to their stem cell content, and we found that enteroids maintained their 3D *in vivo* architecture at both the crypt and mature enteroid stage through 16 passages (roughly 160 culture days) with no phenotypic changes to their 3D architecture (Fig. 1C).

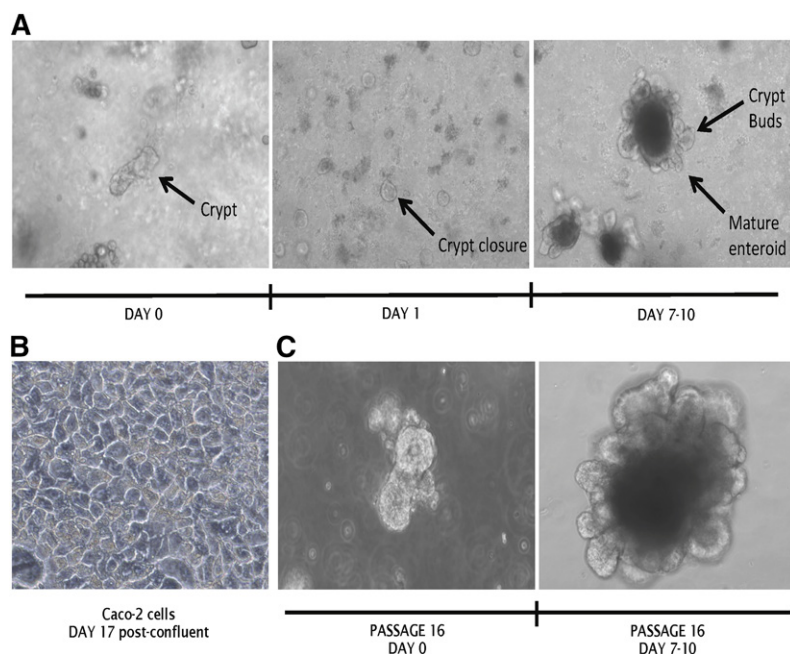


**Fig. 1.** Growth and propagation of primary murine intestinal enteroids. A: Duodenal crypts were plated in 3D culture in Matrigel at day 0 and were provided complete basal growth medium. Crypts reform tight junctions by day 1 and mature enteroids form at days 7–10. B: Caco-2 cells in 2D culture maintained through day 17 post confluence. C: Mature enteroids passaged at maturity 16 times maintain the phenotype of freshly isolated crypts and enteroids. Images were taken at 20× magnification on a Zeiss Axiovert 40C inverted light microscope and are representative of  $n = 12$  unique enteroid lines (all C57Bl/6J WT).

Whereas Caco-2 cells grow in a 2D monolayer composed solely of epithelial cells, mature enteroids are composed of multiple cell types, including stem cells, goblet cells, and enterocytes (17, 23). Compared with freshly isolated intestine (**Fig. 2A**), enteroids significantly decreased markers of terminal epithelial differentiation [brush border villin (VIL1) and enterocyte cytokeratin (KRT)20] from the first day of crypt culture (day 0) through maturation (days 7–10 in culture), though they did not have a significant decrease in enterocyte-specific alkaline phosphatase (ALPI) during this time period. As enteroids matured, they increased their expression of KRT18, a marker of the actively dividing stem cell niche, when compared with whole duodenal tissue expression levels (Fig. 2B). Therefore, enteroid cultures were not composed primarily of enterocytes, but were instead stem cell enriched.

We attempted to drive differentiation within our enterocyte cultures to increase the amount of mature enterocytes that might be capable of secreting chylomicrons. Because Wnt signaling is required for the maintenance of ISCs (24), we withdrew R-spondin from day 6 to day 10 of culture (Fig. 2C) and compared the expression of differentiation markers (as a percent of whole tissue expression levels) between the enteroids maintained in basal growth medium and the differentiated enteroids. Differentiated enteroids

expressed reduced stem cell markers, leucine-rich repeat-containing G protein-coupled receptor 5 (LGR5) and KRT18 (compared with nondifferentiated cells), with concomitant increases in markers of terminal differentiation, including goblet cell marker trefoil factor 3 (TFF3) and KRT20. As shown in Fig. 2D, enterocyte-specific markers were not significantly increased upon differentiation, including ALPI, enterocyte-specific transcription factor Krüppel-like factor 4 (KLF4), VIL1, and brush-border specific sucrase-isomaltase (SI), though their expression trended toward an increase. In all cases, the expression of these genes was normalized to GAPDH, which is expressed uniformly in both undifferentiated and differentiated cells (25).

### Enteroids recapitulate dietary fat absorption, lipoprotein synthesis, and secretion

Previous studies in enteroids have focused on stem cell biology, lineage tracing, and  $\text{Na}^+/\text{H}^+$  exchange (23, 26–28). We asked whether enteroids were able to accomplish TAG absorption, lipoprotein synthesis, and lipoprotein secretion, which are major functions of the intestine. We asked whether key enzymes for dietary FFA and cholesterol absorption, TAG reesterification, and chylomicron synthesis, were present and enriched in mature nondifferentiated enteroids and in differentiated enteroids (**Table 1**). Compared with

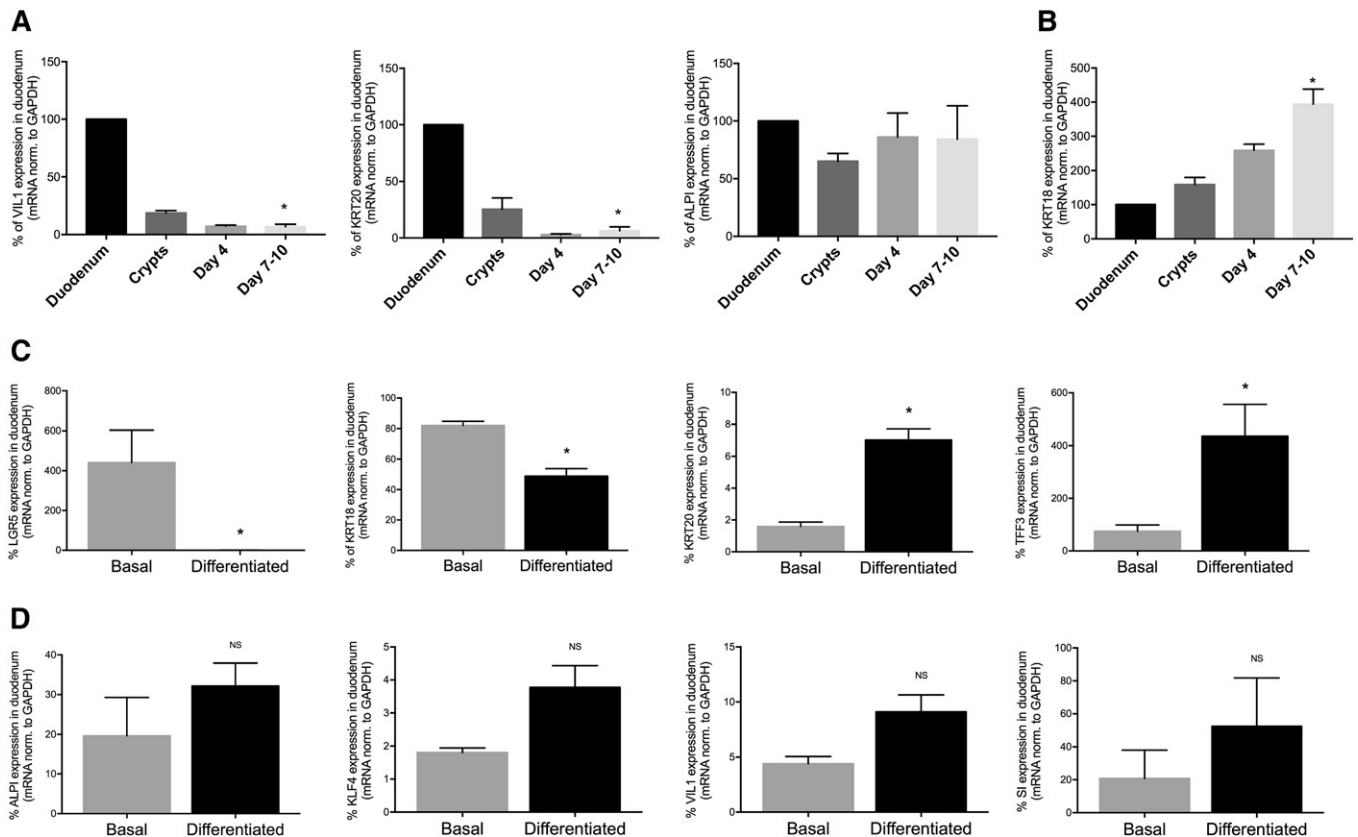


**Fig. 2.** Analysis of differentiation markers of murine duodenal enteroids throughout the culture period. A, B: Percent mRNA expression in whole tissue versus freshly isolated crypts, enteroids in culture for 4 days, and mature enteroids in culture for 7–10 days [ALPI, VIL1, and KRT20 (A) and KRT18 (B)]. Results are mean  $\pm$  SEM. \* $P < 0.05$  compared with duodenum;  $n = 3$ –6 unique enteroid lines (all C57Bl/6J WT). C, D: WT enteroids were grown to maturity in basal growth medium, or differentiated, and differentiation marker mRNA expression was assessed in comparison to whole tissue (100%): LGR5, KRT18, KRT20, and TFF3 (C) and, ALPI, KLF4, VIL1, SI (D). Results are mean  $\pm$  SEM. \* $P < 0.05$  compared with basal enteroids;  $n = 3$ –6 unique enteroid lines (all C57Bl/6J WT).

TABLE 1. Enteroids express key apolipoproteins and enzyme machinery for lipid absorption, synthesis, and secretion

Gene	Basal Enteroid mRNA Expression (% Whole Tissue)	Differentiated Enteroid mRNA Expression (% Whole Tissue)	<i>P</i>
apoA-I	3.72 ± 2.19	20.01 ± 11.77	NS
apoC-III	2.34 ± 0.79	19.23 ± 12.63	NS
apoA-IV	2.34 ± 0.83	13.10 ± 4.60	<0.05 <sup>a</sup>
apoB-48	5.75 ± 3.26	5.12 ± 2.65	NS
CD36	7.68 ± 6.26	11.08 ± 6.03	NS
ACSL5	3.35 ± 1.97	3.30 ± 1.98	NS
FABP2	5.46 ± 2.72	16.98 ± 8.00	NS
ACAT2	5.07 ± 2.40	14.84 ± 6.17	NS
NPC1L1	114.15 ± 65.14	161.05 ± 111.97	NS
MTTP	16.39 ± 10.06	36.39 ± 19.47	NS
MGAT2	12.89 ± 4.13	21.30 ± 4.32	NS
DGAT1	13.55 ± 7.44	34.62 ± 14.85	NS
DGAT2	22.39 ± 14.43	48.83 ± 28.63	NS

mRNA expression is expressed as a percent of mRNA expression in whole duodenum. Results are mean ± SEM; n = 3–6 unique enteroid lines (all C57Bl/6J WT). FABP2, fatty-acid binding protein 2; ACSL5, acyl-CoA synthetase; <sup>a</sup>*P* < 0.05 comparing basal enteroid expression to differentiated expression.

freshly isolated tissue, enteroids had reduced expression of all apolipoprotein mRNA expression under both culture conditions, ranging from ~2 to 20% the level observed in intestine. Differentiation by growth factor withdrawal significantly increased only apoA-IV mRNA expression. Expression of lipid absorption and resynthesis enzymes was also reduced from whole tissue levels, but differentiation of the enteroids only resulted in a trend toward increased expression compared with nondifferentiated enteroids (Table 1). Interestingly, only NPC1L1 was expressed in enteroids (both basal and differentiated) at higher levels than in whole tissue. These data show that enteroids (both basal and differentiated) have the necessary machinery for lipid absorption and chylomicron secretion, but that differentiation does not significantly improve expression levels.

Dietary TAG is absorbed from a proximal-to-distal gradient along the length of the small intestine (29–32). Correspondingly, there is a gradient of terminally differentiated enterocytes responsible for TAG absorption, as well as a gradient of apolipoprotein expression. We asked whether enteroids isolated along the proximal-to-distal gradient would retain this physiological gradient of apolipoprotein expression upon culture and propagation. As shown in Fig. 3A, we cultured enteroids from crypts isolated from duodenum, jejunum, and ileum, and measured apoB-48 mRNA and protein expression (Fig. 3B). apoB-48 expression was highest in duodenal enteroids and decreased along the proximal-to-distal gradient with significantly lower expression in ileal enteroids. Solute carrier family 10 member 2 was expressed in the reverse gradient, and we measured this as both duodenal and ileal tissue and enteroids (Fig. 3B), confirming the maintenance of gene expression along the proximal-to-distal gradient of primary enteroids. In Fig. 3C, D, we confirmed the maintenance of tissue gradient by comparing apoB-48, apoA-IV, and apoA-I mRNA expression in duodenal tissue and to ileal tissue gene expression (Fig. 3C), and found that ileal tissue apolipoprotein expression was ~10% the levels of duodenum. Consistent with these in vivo expression ratios, we found that enteroids cultured to maturity from crypts isolated from duodenum and ileum mirrored this physiological pattern, with ileal

enteroid apolipoprotein expression ranging from ~1 to 10% the levels in duodenal enteroids (Fig. 3D). Therefore, in mature enteroids derived from the most proximal and distal intestine, there was a gradient of apolipoprotein expression that was highest in the duodenum where TAG absorption occurs, and lowest in the ileum where the least TAG absorption occurs; this regional pattern of apolipoprotein expression was maintained through 10 days in culture.

Having established that primary murine enteroid cultures (both nondifferentiated and differentiated) express the key machinery for TAG absorption and lipoprotein synthesis and secretion, we next determined whether this culture model could be used as a model for dietary TAG absorption and chylomicron secretion. As shown in Fig. 4A, confluent Caco-2 cells had significantly more genomic DNA than primary enteroids. This reflected the highly confluent and uniform nature of Caco-2 cells, whereas enteroids grew as a 3D enterocyte-like culture with hollow luminal compartments and large empty areas within the culture dish. Despite the difference in cell number and genomic DNA content, mature enteroids secreted approximately 4-fold more TAG into culture medium (Fig. 4B) than Caco-2 cells maintained for 17 days post confluence (in both high and low glucose media). In vivo, TAG precursors are luminal FFA generated by pancreatic lipase's action on dietary TAG. These FFA precursors are then resynthesized to TAG through the 2-MAG pathway (which is not active in Caco-2 cells, which use the glycerol-3-phosphate pathway). Therefore, we delivered fat to the enteroids in a manner consistent with in vivo fat presentation (to the luminal compartment), a major advantage of the use of primary enteroids as a model in intestinal lipid absorption. We used BODIPY-labeled FA (C12) micelles to demonstrate this luminal delivery to enteroids (Fig. 4C). Mature enteroids were gently opened via pipetting, which exposed the luminal face of the enteroid to BODIPY-FFA micelles. During the initial (0 h) treatment, both the inner lumen and the basolateral side of the enteroids were exposed to lipid, with fluorescence in and around the mature enteroid. After 1 h, the enteroids reclosed and at 2 h were stringently washed to

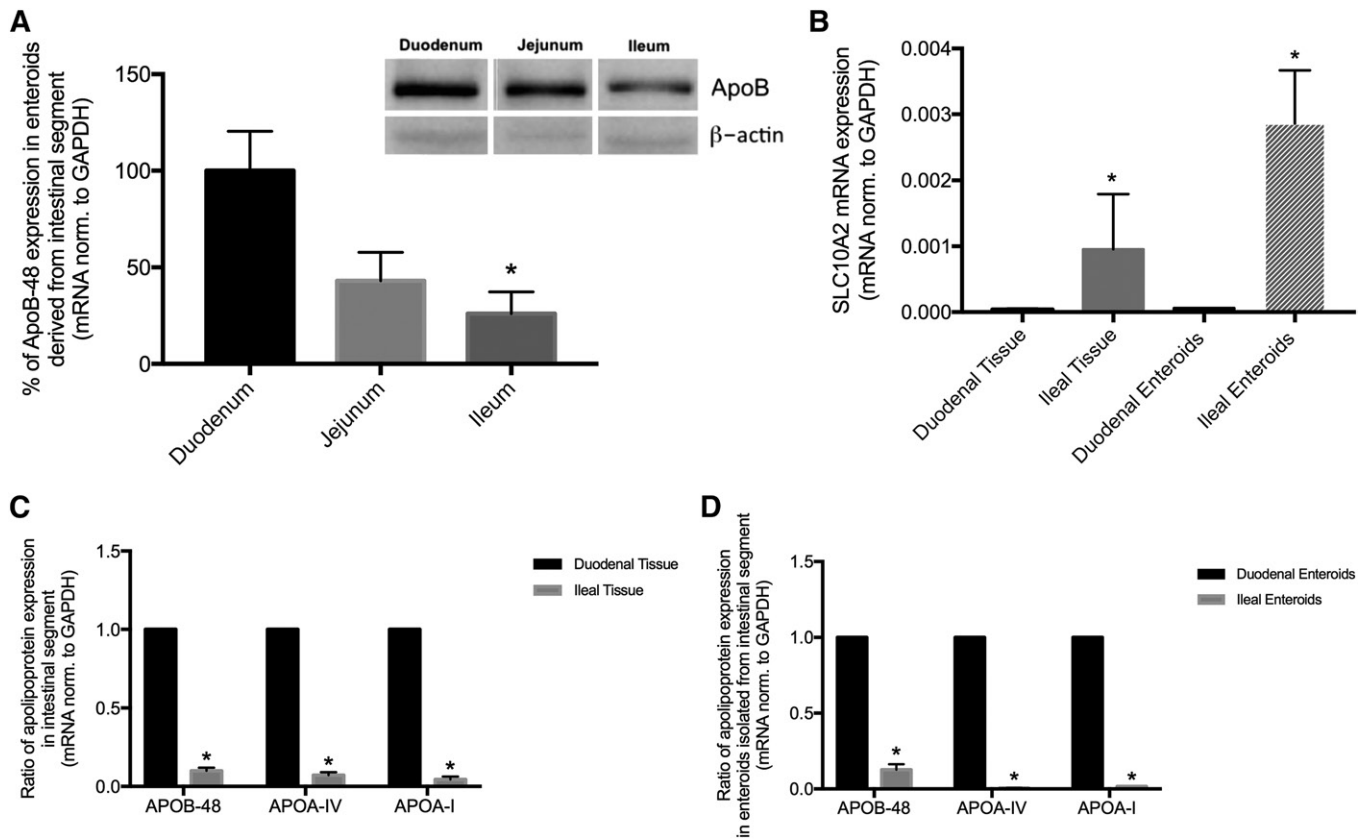


**Fig. 3.** Enteroids maintain regional gene expression characteristics of their tissue of origin. **A:** mRNA and protein expression for apoB-48 in mature enteroids established from duodenal, jejunal, or ileal crypts. Inset: Protein expression of intracellular apoB-48.  $*P < 0.05$  in comparison to duodenal enteroids;  $n = 3-6$  unique enteroid lines (all C57Bl/6J WT). **B:** Solute carrier family 10 member 2 (SLC10A2). **C:** Fold change analysis of apolipoprotein expression in freshly isolated duodenal tissue to ileal tissue. **D:** Fold change analysis of apolipoprotein expression in mature enteroids derived from either duodenum or ileum. Results are mean  $\pm$  SEM.  $*P < 0.05$ ;  $n = 3-6$  unique enteroid lines (all C57Bl/6J WT).

remove micelles from the basolateral surface. After 2 h of treatment and washing, all remaining BODIPY fluorescence was present in the lumen of the enteroid, rather than on the basolateral surface. After another 4–6 h, we removed the medium containing secreted lipoproteins (not shown). Though this approach did not fully approximate dietary fat absorption, it did significantly enrich the amount of lipid that was presented to luminal face of the enteroids. This experimental approach simulated availability (in micelles or as FFA bound to BSA) and presentation (to the luminal surface) of dietary lipid. We could not discount any lipid that was taken up from the basolateral surface during the first 2 h incubation, however. Using this approach, we assessed whether enteroids were able to re-esterify [ $^3$ H]FFA delivered to the lumen into cellular and secreted [ $^3$ H]TAG (Fig. 4D). We found that  $\sim 1.0\%$  of the [ $^3$ H]FFA dose was incorporated into the cellular TAG pool and  $\sim 0.5\%$  of the [ $^3$ H]FFA dose was secreted from the enteroids into the medium as [ $^3$ H]TAG. Differentiation did not significantly increase the  $\sim 1.5\%$  of the [ $^3$ H]FFA dose that was incorporated into [ $^3$ H]TAG (Fig. 4E). The secretion of TAG from enteroids occurred concomitantly with both apoA-IV and apoB-48 into the culture medium (Fig. 4E, inset), which reflects apolipoprotein and chylomicron secretion in vivo.

Compared with post confluent Caco-2 cells (Fig. 4F), the rate of TAG secretion in response to a dose of BSA-bound OA was significantly lower in enteroids, even after adjusting for cell number via genomic DNA content. Though cell culture models often use BSA-bound FFA as a delivery method, this does not exactly approximate dietary lipid absorption, which involves the concomitant absorption of FFA, MAG, cholesterol, and phospholipids in bile acid mixed micelles. Therefore, we compared [ $^3$ H]TAG secretion when the labeled [ $^3$ H]FFA was delivered in mixed micelles. As shown in Fig. 4G, we found that this stimulated [ $^3$ H]TAG secretion from enteroids and that, compared with Caco-2 cells, treatment with mixed micelles in enteroids resulted in a  $\sim 4$ -fold increase in TAG secretion. Enteroids were also able to absorb [ $^{14}$ C]cholesterol, and that cholesterol was incorporated into the cellular compartment after a 6 h incubation (Fig. 4H).

In vivo, the intestine secretes dietary lipid in a chylomicron particle. When we treated enteroids with BSA or OA bound to BSA (Fig. 5B), we found that enteroids secreted chylomicron-sized particles and that OA treatment significantly increased the average size from  $\sim 100$  to 125 nm, which is consistent with chylomicrons isolated from lymph, which range from 100 to 350 nm (33–35). In contrast, Caco-2



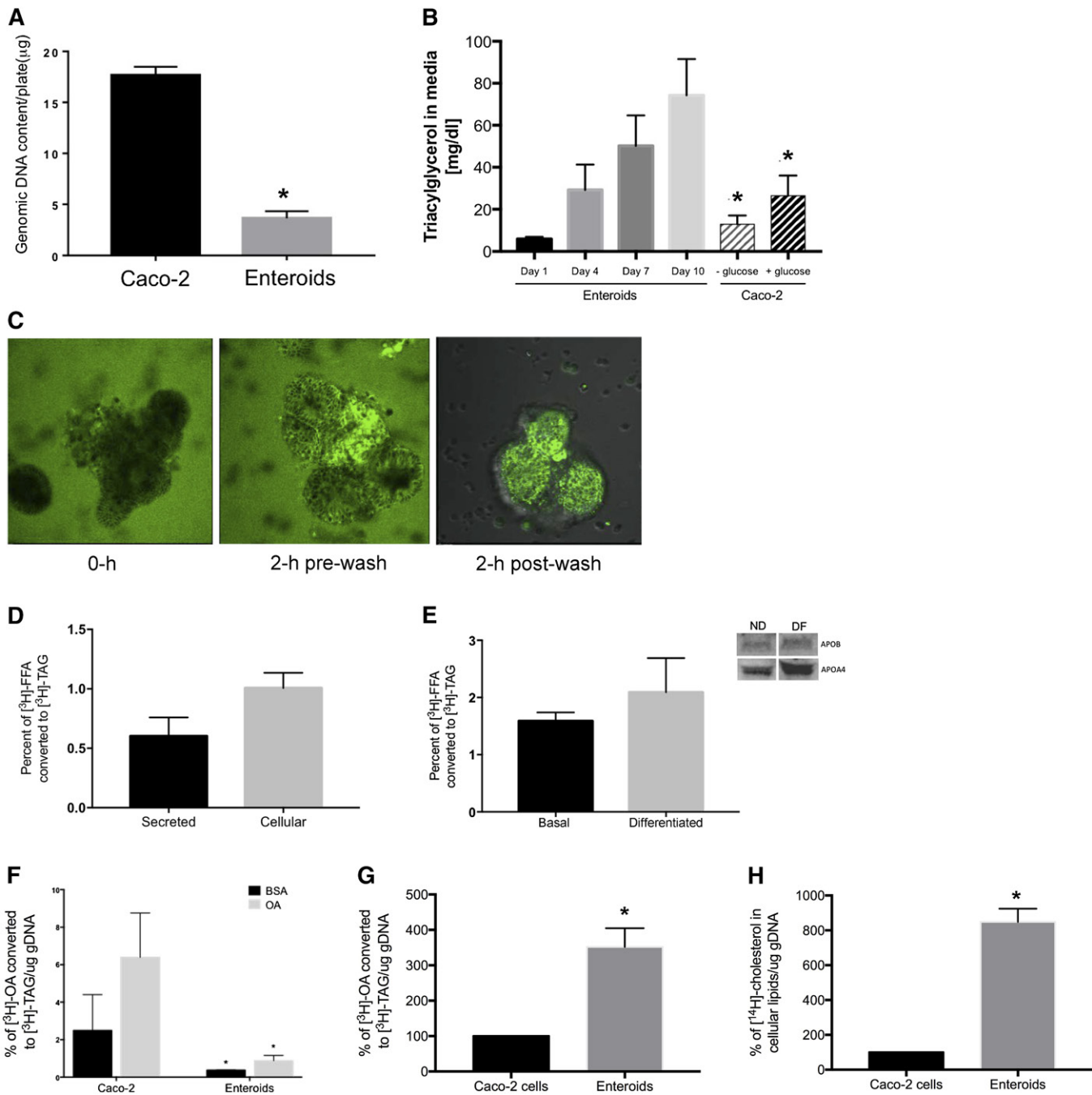


**Fig. 4.** Enteroids synthesize and secrete TAG from FA precursors. **A:** Genomic DNA content of parallel cultures of Caco-2 cells and enteroids. **B:** Secretion of TAG into media from nondifferentiated enteroid cultures and 17 day post confluent Caco-2 cells. **C:** Incorporation of BODIPY-C12 FFA into enteroid lumen during 2 h treatment with BODIPY-FFA micelles. **D:** Enteroids were treated with 400  $\mu$ M OA:BSA or BSA alone, and 0.5  $\mu$ Ci [ $^3$ H]OA and the conversion to [ $^3$ H]TAG was assessed after Folch extraction in both the media and the cellular lipid contents. **E:** Enteroids were cultured under basal and differentiated conditions and treated with lipid as in (D). **F:** Enteroids and Caco-2 cells were treated as in (D) and total [ $^3$ H]TAG in media and cells was assessed. Enteroids and Caco-2 cells were treated with mixed micelles containing [ $^3$ H]OA (G) and [ $^{14}$ C]cholesterol (H), and TAG and cholesterol accumulation was measured after Folch extraction. Results are mean  $\pm$  SEM. \* $P$  < 0.05, comparing Caco-2 to day 10 enteroids [as in (B)], comparing enteroids to Caco-2 with same treatment (F);  $n$  = 3 unique enteroid lines (all C57Bl/6J WT).

monolayers secreted  $\sim$ 25 nm lipoproteins, consistent with the known secretion pattern VLDL, HDL, and LDL, rather than chylomicron-sized particles. We isolated secreted lipoproteins from Caco-2 cells and primary enteroids treated identically with growth medium (Fig. 5C) that were significantly smaller.

#### Intestine-specific overexpression of apoC-III inhibits dietary fat absorption and results in the secretion of smaller chylomicrons

Finally, we wanted to determine whether primary enteroids, as a culture model for intestinal dietary fat absorption, would maintain the defects in intestinal lipid



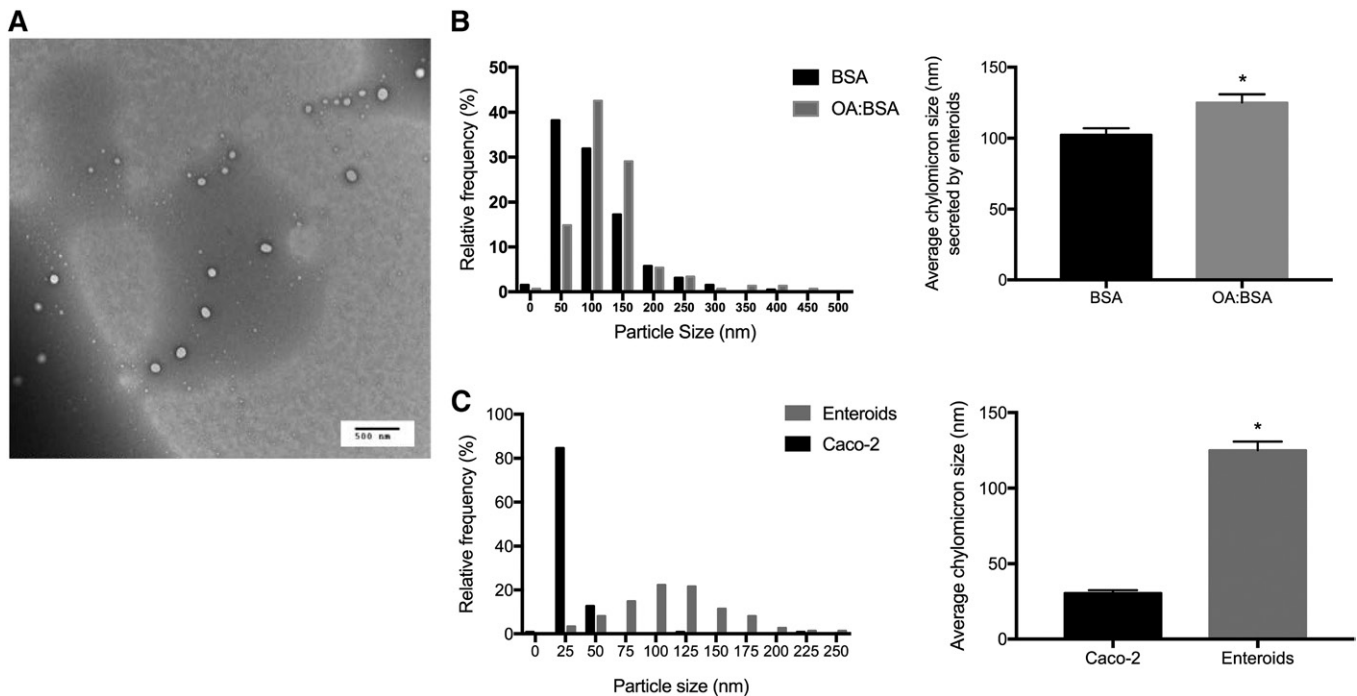


**Fig. 5.** Enteroids secrete a chylomicron-sized particle. A: Chylomicrons were isolated by ultracentrifugation followed by TEM, representative TEM image ( $n = 3-6$  unique enteroid lines). B: Mature enteroids were treated with either 400  $\mu\text{M}$  OA:BSA or BSA control for 6 h; lipoproteins were isolated and sized. C: The TEM sizes of lipoproteins secreted from mature nondifferentiated enteroids were compared with lipoproteins secreted from Caco-2 cells treated with 400  $\mu\text{M}$  OA. Results are mean  $\pm$  SEM. \* $P < 0.05$ ;  $n = 3$  different enteroid lines (all C57Bl/6J WT); 200–600 particles were counted per group.

absorption and secretion that are observed in *in vivo* mouse models. Hu-apoC-III Tg mice have a defect in dietary lipid absorption resulting in a delay in chylomicron secretion (14); we asked whether primary enteroids derived from hu-apoC-III Tg mice retained this defect. As shown in **Fig. 6A**, enteroids derived from WT mice expressed no human apoC-III mRNA, whereas enteroids derived from hu-apoC-III Tg mice expressed the human form of apoC-III. Hu-apoC-III Tg enteroids secreted significantly less TAG into the culture medium at days 4–10 of the culture period, when compared directly to parallel enteroid cultures of WT enteroids (**Fig. 6B**). Cells were treated with mixed micelles containing [ $^3\text{H}$ ]FFA, and the rate of incorporation of that [ $^3\text{H}$ ]FFA into the [ $^3\text{H}$ ]TAG pool was determined; we found that hu-apoC-III Tg enteroids had a reduced rate of [ $^3\text{H}$ ]TAG accumulation (both intracellularly and secreted) compared to WT enteroids (**Fig. 6C**). Hu-apoC-III Tg enteroids secreted smaller chylomicrons than their WT counterparts, with an average chylomicron size of  $\sim 50$  nm, compared with the  $\sim 100$  nm chylomicrons secreted by WT enteroids under basal growth conditions (**Fig. 6D**). This decrease in chylomicron size and TAG secretion may be due to a decrease in FFA incorporation into TAG in the enterocyte. We found that CD36, a plasma membrane FA transporter, was significantly reduced in the hu-apoC-III Tg enteroids (compared with WT enteroids). *In vivo*, CD36 deficiency impairs chylomicron secretion (49), suggesting that the chylomicron secretion defect in apoC-III overexpressing intestine may be due to this reduced CD36 expression. Most importantly, this defect in TAG secretion and

CD36 expression occurs in the absence of feedback from the liver, since these cultured enteroids are not receiving any basolateral signals from blood.

## DISCUSSION

We report here that primary murine enteroids recapitulate dietary fat absorption, secrete a chylomicron-sized particle, mirror intestinal absorption defects present in the genetic background of the mouse the enteroids are isolated from, and can be exploited to discern key intestinal mechanisms directly applicable to disease.

The use of primary enteroids in culture has significant advantages. First, these cells maintain their *in vivo* orientation with an apical surface facing inwards around a central lumen, and a basolateral surface facing outwards toward the medium/extracellular matrix. The presence of ISCs in the enteroid culture allows the enteroids to be expanded and passaged in culture indefinitely. Like the intact intestine, the enteroid crypts expand in culture by sloughing off cells into the luminal compartment followed by regeneration of crypt epithelium. These cultures can be genetically manipulated to study overexpression and knockdown of key intestinal genes (18). This last point is not minor; primary mouse enterocytes are not viable in culture long enough for these types of studies, and human epithelial colorectal adenocarcinoma cells (Caco-2) cells do not fully retain *in vivo* physiology because they are a transformed culture system that grows in a monolayer sheet rather than

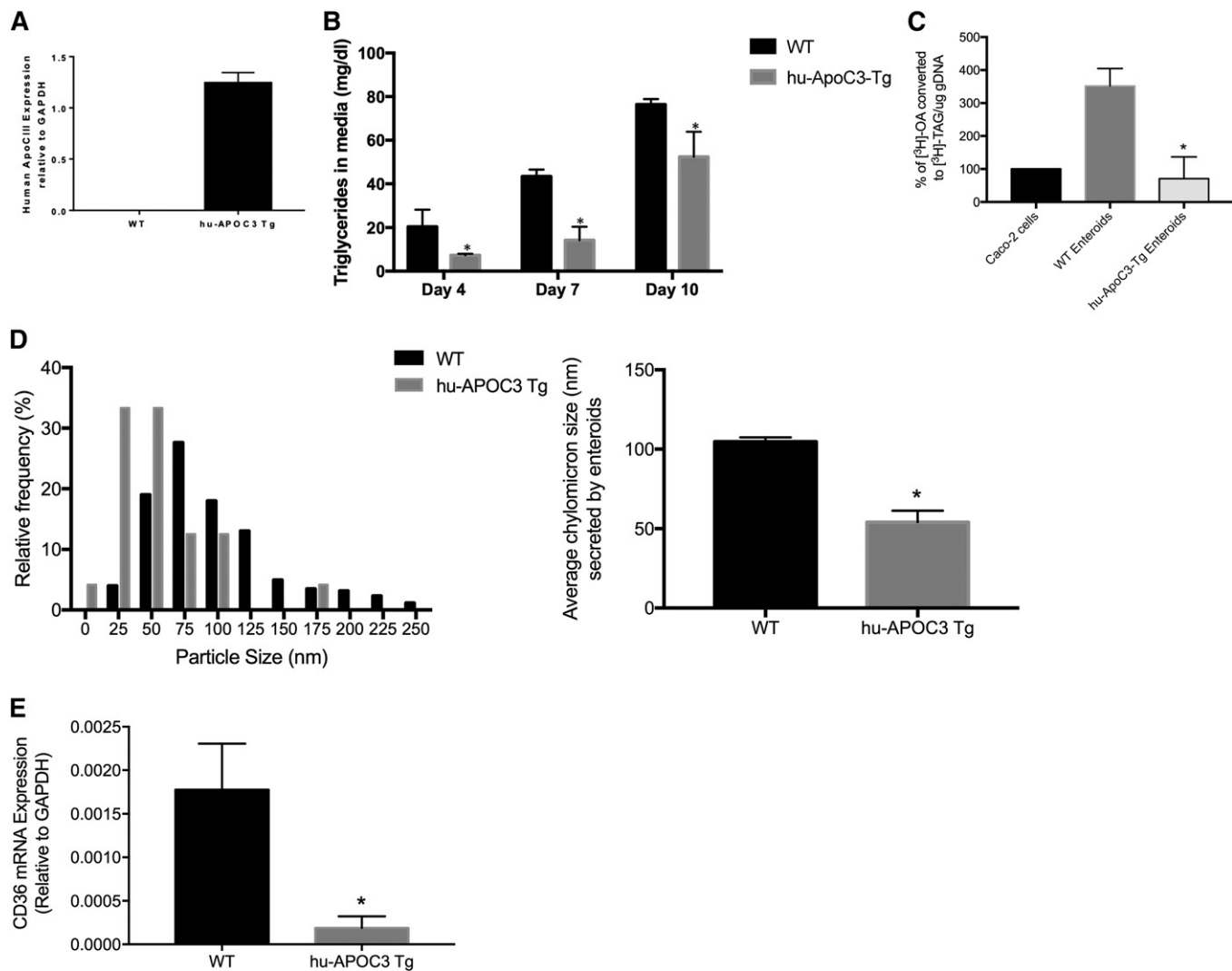


**Fig. 6.** Enteroids derived from hu-apoC-III Tg mice secrete less TAG and smaller chylomicrons. **A:** Enteroids derived from hu-apoC-III Tg mice express human apoC-III mRNA, WT enteroids do not. **B:** Basal secretion of TAG into media. **C:** Enteroids and Caco-2 cells were treated with mixed micelles containing [ $^3$ H]OA and the rate of TAG accumulation was measured after Folch extraction (and compared directly to rate at which Caco-2 cells accumulate [ $^3$ H]TAG. Results are mean  $\pm$  SEM. \* $P < 0.05$ , comparing WT to hu-apoC-III Tg enteroids. **D:** Chylomicrons were isolated and sized as in Fig. 5B. **E:** Relative CD36 mRNA expression in WT and hu-apoC-III Tg enteroids. Results are mean  $\pm$  SEM. \* $P < 0.05$ ;  $n = 3$ –6 unique enteroid lines for WT and transgenic mice.

around a central lumen. Everted gut sacs, another option for ex vivo mechanistic studies, cannot be genetically manipulated due to their short viability. It should be noted that the lymph fistula mouse model is still the gold standard for in vivo physiology of dietary fat absorption and enteroendocrine secretions. However, lymph fistula studies (and the everted gut sac model) cannot be maintained indefinitely, with a maximum experimental time of 8 and 24 h, respectively. We show that enteroids maintain in vivo characteristics throughout 16 passages with no change.

When compared with established models of dietary fat absorption, primary murine enteroids have several key strengths. In vivo, the intestinal epithelium is in a constant state of differentiation, renewal, and replacement, driven by the crypt-villus axis, which makes up the functional unit of the intestine. In the crypt, long-lived multi-potent stem cells (the ISCs) expressing LGR5 give rise to all the cells lining the intestinal epithelium. LGR5-positive cells are

highly dependent on Wnt signaling, which was stimulated by R-spondin in our cultures. We tried a variety of growth factor withdrawal approaches to push the cultures toward a terminally differentiated state containing a higher ratio of mature enterocytes (data not shown), including our differentiation protocol where R-spondin was removed, and had varying degrees of success. Ultimately, R-spondin removal results in a higher amount of terminally differentiated cells, but this comes at the cost of LGR5+ niche, which means that replenishment of differentiated epithelial cells is lost. It has recently been reported that there is an additional niche of differentiated epithelial enterocytes that reverts to multipotent ISCs when LGR5+ stem cells are ablated (28, 36). This may explain one of the significant issues we faced with our primary enteroid cultures, which stubbornly retained “stem-ness” and high expression of LGR5 throughout culture. In order to create a more enterocyte-lineage-committed culture, we needed to select for

differentiation rather than support the stem cell niche, through genetic approaches [including the approach used by Clevers et al. (7) to transiently ablate LGR5+ cells or alternatively by knocking down *Math1* to reduce signaling through the Notch pathway (5, 6, 37)]. Ultimately, we decided that retention of the secretory and stem cells was a major advantage of the enteroid system, and that these genetic approaches might yield a more enterocyte-enriched culture, but not a more physiologic model. Existing approaches to cultures of primary enterocytes have a finite *ex vivo* lifespan, so we did not ultimately pursue this approach.

We found that enteroids derived from specific regions within the intestine maintained the physiological aspects of their tissue of origin and mirrored the absorptive phenotype of the absorptive gradient along the intact tissue. Specifically, treatment of proximal enteroids (duodenum) resulted in the highest rate of chylomicron secretion, coupled with high apoB mRNA expression. Conversely, enteroids cultured from crypts isolated from the distal intestine (ileum) had the lowest rate of chylomicron secretion in response to FA. Based on this tissue organization, it was likely that these ileal enteroids would be effective for studies of bile acid metabolism. Our data demonstrate that enteroids retain differentiated epithelial characteristics and mimic the native tissue physiology. An important unanswered question in our hands is the extent to which these cultures secrete incretin hormones and other endocrine secretions. Though we have shown that enteroids reflect key characteristics of their tissue of origin, whether they retain specific changes resulting from an *in vivo* milieu of metabolic disease is unknown (for example, altered gene expression when coming from diet-induced diabetes models).

We confirmed that LGR5+ stem cells also express apoB (29). We believe the mature enterocytes expressing ALPI are the most responsible for chylomicron secretion, however, because it is only after mature enterocytes appear that significant TAG secretion occurs.

A limitation of this organoid system, as for other reported tissue organoids (23, 38, 39), is that our enteroid models cannot exactly recapitulate the *in vivo* tissue. As we have demonstrated, although the cellular lineage composition, polarity around a central lumen, and stimulation by FFA mimic *in vivo* tissue physiology, there are several key aspects of the *in vivo* environment that are lacking. First, the underlying neuromuscular architecture is lost in enteroid culture. Because neural input is integral to many gastrointestinal functions, including peristalsis, endocrine secretion, and gastric emptying into the duodenum, this is a fundamental drawback of this culture system. Second, the intestinal lymphatics are lacking, which means that enteroids cannot recapitulate a key aspect of intestinal physiology where dietary long chain FAs are transported through the lymph, prior to entering the plasma through the right subclavian vein (40). Finally, we found that enteroids secrete TAG at a lower rate from FFA precursors than Caco-2 cell cultures. This is likely because the enteroid cultures contain fewer epithelial cells (and total cells in general) than monolayer Caco-2 cultures. This may also be due to the exclusive use of the liver-specific glycerol-3-phosphate


pathway by Caco-2 cells; a pathway that is normally used to assemble VLDL. In contrast, enteroids use the intestinal 2-MAG pathway (as measured by TAG secretion and mRNA expression), which is preferred by enterocytes *in vivo*. When we delivered FFA within MAG-containing mixed micelles (as in Fig. 4), this was apparent in the increase in the rate at which enteroids converted that FFA, likely shunted through the MAG pathway, into labeled TAG versus Caco-2 cells, which should be less able to utilize this type of FFA substrate. Another limitation is that the rate of TAG secretion is quite low (~1.5%) in primary enteroids. This could be due to the short dosing period (to reduce the time the enteroids are in suspension culture); it could be due to the addition of Rho-kinase inhibitor to prevent suspension-related apoptosis; and it could also be due to the retention of the LGR5+ cells at the expense of epithelial cells. Enteroids maintained in complete growth medium still secrete TAG, which suggests that they are using acyl precursors derived from a different pool than during treatment with OA. This is another difference between *in vivo* enterocytes and the enteroid cultures.

The enteroid model described here facilitated studies of apoC-III overexpression in intestine. Recent epidemiological studies show that apoC-III is an independent predictor of CVD risk and progression in humans (9, 40, 41), and that its presence on lipoproteins promotes their atherogenicity (8, 43–45). This is likely because apoC-III, expressed in both liver and the intestine, raises plasma TAG through the inhibition of hepatic clearance of TAG-rich chylomicrons and VLDLs, stimulates VLDL secretion, and modulates intestinal TAG trafficking (12, 46–48).

We show for the first time that apoC-III plays an intestine-specific role in mediating fat metabolism. Prior to the development of this model, a major burden in these studies was in isolating the effects of altered intestinal chylomicron secretion from alterations in both plasma lipids and hepatic uptake and synthesis. A major issue was the confounding effect of apoC-III present in bile secretions from the liver, coupled with potential feedback inhibition on chylomicron secretion by the hypertriglyceridemia found in apoC-III Tg mice (~500–800 mg/dl). We found that overexpression of apoC-III in primary murine enteroids results in reduced lipoprotein secretion in the absence of basolateral exposure to raised plasma TAG, or endocrine feedback from the liver through plasma or bile. apoC-III overexpression in primary murine enteroids also resulted in the secretion of smaller chylomicrons, containing significantly less dietary TAG. We measured CD36 expression, because it is a major regulator of intestinal lipoprotein secretion, and we found that in the absence of hepatic feedback, CD36 is reduced in hu-apoC-III Tg enteroids. The enteroid culture model presented here, therefore, is not only appropriate for modeling key aspects of dietary fat absorption, but is also potentially critical for determining intestinal mechanisms where lack of hepatic secretions are critical (1, 49).

The intestinal enteroid model represents a significant advance in our ability to determine intestinal mechanisms for dietary fat absorption and lipoprotein synthesis and



secretion, as well as to determine mechanisms for intestinal regulators of metabolic disease, including apoC-III. This model will significantly expand our ability to test how specific genes or genetic polymorphisms function in dietary fat absorption and the precise intestinal mechanisms that are critical in the etiology of metabolic disease. 

This work was performed in part at the Biosciences Electron Microscopy Facility of the University of Connecticut, and the authors would specifically like to thank Dr. Xuanhao Sun.

## REFERENCES

- Tomkin, G. H., and D. Owens. 2012. The chylomicron: relationship to atherosclerosis. *Int. J. Vasc. Med.* **2012**: 784536.
- Lai, C-Q., L. D. Parnell, and J. M. Ordovas. 2005. The APOA1/C3/A4/A5 gene cluster, lipid metabolism and cardiovascular disease risk. *Curr. Opin. Lipidol.* **16**: 153–166.
- Pan, X., and M. M. Hussain. 2012. Gut triglyceride production. *Biochim. Biophys. Acta.* **1821**: 727–735.
- Mansbach 2nd, C. M., and F. Gorelick. 2007. Development and physiological regulation of intestinal lipid absorption. II. Dietary lipid absorption, complex lipid synthesis, and the intracellular packaging and secretion of chylomicrons. *Am. J. Physiol. Gastrointest. Liver Physiol.* **293**: G645–G650.
- Date, S., and T. Sato. 2015. Mini-gut organoids: reconstitution of the stem cell niche. *Annu. Rev. Cell Dev. Biol.* **31**: 269–289.
- VanDussen, K. L., A. J. Carulli, T. M. Keeley, S. R. Patel, B. J. Puthoff, S. T. Magness, I. T. Tran, I. Maillard, C. Siebel, Å. Kolterud, et al. 2012. Notch signaling modulates proliferation and differentiation of intestinal crypt base columnar stem cells. *Development.* **139**: 488–497.
- Sato, T., R. G. Vries, H. J. Snippert, M. van de Wetering, N. Barker, D. E. Stange, J. H. van Es, A. Abo, P. Kujala, P. J. Peters, et al. 2009. Single Lgr5 stem cells build crypt-villus structures in vitro without a mesenchymal niche. *Nature.* **459**: 262–265.
- Sacks, F. M., P. Alaupovic, L. a. Moye, T. G. Cole, B. Sussex, M. J. Stampfer, M. a. Pfeffer, and E. Braunwald. 2000. VLDL, apolipoproteins B, CIII, and E, and risk of recurrent coronary events in the Cholesterol and Recurrent Events (CARE) trial. *Circulation.* **102**: 1886–1892.
- Qamar, A., S. A. Khetarpal, A. V. Khera, A. Qasim, D. J. Rader, and M. P. Reilly. 2015. Plasma apolipoprotein C-III levels, triglycerides, and coronary artery calcification in type 2 diabetics. *Arterioscler. Thromb. Vasc. Biol.* **35**: 1880–1888.
- Olivieri, O., C. Stranieri, A. Bassi, B. Zaia, D. Girelli, F. Pizzolo, E. Trabetti, S. Cheng, M. A. Grow, P. F. Pignatti, et al. 2002. ApoC-III gene polymorphisms and risk of coronary artery disease. *J. Lipid Res.* **43**: 1450–1457.
- Zheng, C., C. Khoo, J. Furtado, and F. M. Sacks. 2010. Apolipoprotein C-III and the metabolic basis for hypertriglyceridemia and the dense low-density lipoprotein phenotype. *Circulation.* **121**: 1722–1734.
- Zhong, S., M. B. Khalil, P. H. Links, Y. Zhao, J. Iqbal, M. Hussain, R. J. Parks, Y. Wang, and Z. Yao. 2010. Expression of apolipoprotein C-III in McA-RH7777 cells enhances VLDL assembly and secretion under lipid-rich conditions. *J. Lipid Res.* **51**: 150–161.
- Yao, Z., and Y. Wang. 2012. Apolipoprotein C-III and hepatic triglyceride-rich lipoprotein production. *Curr. Opin. Lipidol.* **23**: 206–212.
- Wang, F., A. B. Kohan, H. H. Dong, Q. Yang, M. Xu, S. Huesman, D. Lou, D. Y. Hui, and P. Tso. 2014. Overexpression of apolipoprotein C-III decreases secretion of dietary triglyceride into lymph. *Physiol. Rep.* **2**: e00247.
- Tso, P., D. S. Drake, D. D. Black, and S. M. Sabesin. 1984. Evidence for separate pathways of chylomicron and very low-density lipoprotein assembly and transport by rat small intestine. *Am. J. Physiol.* **247**: G599–G610.
- Altomonte, J., L. Cong, S. Harbaran, A. Richter, J. Xu, M. Meseck, and H. H. Dong. 2004. Foxo1 mediates insulin action on apoC-III and triglyceride metabolism. *J. Clin. Invest.* **114**: 1493–1503.
- Mahe, M. M., N. Sundaram, C. L. Watson, N. F. Shroyer, and M. A. Helmrath. 2015. Establishment of human epithelial enteroids and colonoids from whole tissue and biopsy. *J. Vis. Exp.* **97**: e52483–e52496.
- Van Lidh de Jeude, J. F., J. L. Vermeulen, P. S. Montenegro-Miranda, G. R. Van den Brink, and J. Heijmans. 2015. A protocol for lentiviral transduction and downstream analysis of intestinal organoids. *J. Vis. Exp.* **98**: 52531.
- Kohan, A. B., Y. Qing, H. A. Cyphert, P. Tso, and L. M. Salati. 2011. Chylomicron remnants and nonesterified fatty acids differ in their ability to inhibit genes involved in lipogenesis in rats. *J. Nutr.* **141**: 171–176.
- Nauli, A. M., Y. Sun, J. D. Whittimore, S. Atyia, G. Krishnaswamy, and S. M. Nauli. 2014. Chylomicrons produced by Caco-2 cells contained ApoB-48 with diameter of 80-200 nm. *Physiol. Rep.* **2**: 192–196.
- Kohan, A. B., F. Wang, X. Li, S. Bradshaw, Q. Yang, J. L. Caldwell, T. M. Bullock, and P. Tso. 2012. Apolipoprotein A-IV regulates chylomicron metabolism-mechanism and function. *Am. J. Physiol. Gastrointest. Liver Physiol.* **302**: G628–G636.
- Folch, J., M. Lees, and G. H. Sloane Stanley. 1957. A simple method for the isolation and purification of total lipides from animal tissues. *J. Biol. Chem.* **226**: 497–509.
- Foulke-Abel, J., J. In, J. Yin, N. C. Zachos, O. Kovbasnjuk, M. K. Estes, H. de Jonge, and M. Donowitz. 2016. Human enteroids as a model of upper small intestinal ion transport physiology and pathophysiology. *Gastroenterology.* **150**: 638–649.e8.
- Fevr, T., S. Robine, D. Louvard, and J. Huelsken. 2007. Wnt/beta-catenin is essential for intestinal homeostasis and maintenance of intestinal stem cells. *Mol. Cell. Biol.* **27**: 7551–7559.
- Murphy, C. L., and J. M. Polak. 2002. Differentiating embryonic stem cells: GAPDH, but neither HPRT nor beta-tubulin is suitable as an internal standard for measuring RNA levels. *Tissue Eng.* **8**: 551–559.
- Jabaji, Z., C. M. Sears, G. J. Brinkley, N. Y. Lei, V. S. Joshi, J. Wang, M. Lewis, M. Stelzner, M. G. Martín, and J. C. Y. Dunn. 2013. Use of collagen gel as an alternative extracellular matrix for the in vitro and in vivo growth of murine small intestinal epithelium. *Tissue Eng. Part C Methods.* **19**: 961–969.
- Jabaji, Z., G. J. Brinkley, H. A. Khalil, C. M. Sears, N. Y. Lei, M. Lewis, M. Stelzner, M. G. Martín, and J. C. Dunn. 2014. Type I collagen as an extracellular matrix for the in vitro growth of human small intestinal epithelium. *PLoS One.* **9**: e107814.
- Tetteh, P. W., O. Basak, H. F. Farin, K. Wiebrands, K. Kretzschmar, H. Begthel, M. Van Den Born, J. Korving, F. De Sauvage, J. H. Van Es, et al. 2016. Replacement of lost Lgr5-positive stem cells through plasticity of their enterocyte-lineage daughters. *Cell Stem Cell.* **18**: 203–213.
- Levy, E., J. F. Beaulieu, E. Delvin, E. Seidman, W. Yotov, J. R. Basque, and D. Ménard. 2000. Human crypt intestinal epithelial cells are capable of lipid production, apolipoprotein synthesis, and lipoprotein assembly. *J. Lipid Res.* **41**: 12–22.
- Simon, T., V. R. Cook, A. Rao, and R. B. Weinberg. 2011. Impact of murine intestinal apolipoprotein A-IV expression on regional lipid absorption, gene expression, and growth. *J. Lipid Res.* **52**: 1984–1994.
- Thomson, A. B., M. Keelan, M. L. Garg, and M. T. Clandinin. 1989. Intestinal aspects of lipid absorption: in review. *Can. J. Physiol. Pharmacol.* **67**: 179–191.
- Black, D. D. 2007. Development and physiological regulation of intestinal lipid absorption. I. Development of intestinal lipid absorption: cellular events in chylomicron assembly and secretion. *Am. J. Physiol. Gastrointest. Liver Physiol.* **293**: G519–G524.
- Sabesin, S. M., and S. Frase. 1977. Electron microscopic studies of the assembly, intracellular transport, and secretion of chylomicrons by rat intestine. *J. Lipid Res.* **18**: 496–511.
- Martins, I. J., B. C. Mortimer, J. Miller, and T. G. Redgrave. 1996. Effects of particle size and number on the plasma clearance of chylomicrons and remnants. *J. Lipid Res.* **37**: 2696–2705.
- Kohan, A. B., F. Wang, X. Li, A. E. Vandarsall, S. Huesman, M. Xu, Q. Yang, D. Lou, and P. Tso. 2013. Is apolipoprotein A-IV rate limiting in the intestinal transport and absorption of triglyceride? *Am. J. Physiol. Gastrointest. Liver Physiol.* **304**: G1128–G1135.
- Drover, V. A., M. Ajmal, F. Nassir, N. O. Davidson, A. M. Nauli, D. Sahoo, P. Tso, and N. A. Abumrad. 2005. CD36 deficiency impairs intestinal lipid secretion and clearance of chylomicrons from the blood. *J. Clin. Invest.* **115**: 1290–1297.
- Yan, K. S., L. A. Chia, X. Li, A. Ootani, J. Su, J. Y. Lee, N. Su, Y. Luo, S. C. Heilshorn, M. R. Amieva, et al. 2012. The intestinal stem cell markers Bmi1 and Lgr5 identify two functionally distinct populations. *Proc. Natl. Acad. Sci. USA.* **109**: 466–471.

38. Schumacher, M. A., E. Aihara, R. Feng, A. Engevik, N. F. Shroyer, K. M. Ottemann, R. T. Worrell, M. H. Montrose, R. A. Shivdasani, and Y. Zavros. 2015. The use of murine-derived fundic organoids in studies of gastric physiology. *J. Physiol.* **593**: 1809–1827.
39. Stange, D. E., B-K. Koo, M. Huch, G. Sibbel, O. Basak, A. Lyubimova, P. Kujala, S. Bartfeld, J. Koster, J. H. Geahlen, et al. 2013. Differentiated Troy+ chief cells act as reserve stem cells to generate all lineages of the stomach epithelium. *Cell.* **155**: 357–368.
40. Swartz, M. A. 2001. The physiology of the lymphatic system. *Adv. Drug Deliv. Rev.* **50**: 3–20.
41. Crosby, J., G. M. Peloso, P. L. Auer, D. R. Crosslin, N. O. Stitzel, L. A. Lange, Y. Lu, Z. Tang, H. Zhang, G. Hindy, et al. 2014. Loss-of-function mutations in APOC3, triglycerides, and coronary disease. *N. Engl. J. Med.* **371**: 22–31.
42. Onat, A., G. Hergenç, V. Sansoy, M. Fobker, K. Ceyhan, S. Toprak, and G. Assmann. 2003. Apolipoprotein C-III, a strong discriminant of coronary risk in men and a determinant of the metabolic syndrome in both genders. *Atherosclerosis.* **168**: 81–89.
43. Talayero, B., L. Wang, J. Furtado, V. J. Carey, G. A. Bray, and F. M. Sacks. 2014. Obesity favors apolipoprotein E- and C-III-containing high density lipoprotein subfractions associated with risk of heart disease. *J. Lipid Res.* **55**: 2167–2177.
44. Jensen, M. K., E. B. Rimm, J. D. Furtado, and F. M. Sacks. 2012. Apolipoprotein C-III as a potential modulator of the association between HDL-cholesterol and incident coronary heart disease. *J. Am. Heart Assoc.* **1**: 1–10.
45. Lee, S. J., H. Campos, L. A. Moye, and F. M. Sacks. 2003. LDL containing apolipoprotein CIII is an independent risk factor for coronary events in diabetic patients. *Arterioscler. Thromb. Vasc. Biol.* **23**: 853–858.
46. Breyer, E. D., N. A. Le, X. Li, D. Martinson, and W. V. Brown. 1999. Apolipoprotein C-III displacement of apolipoprotein E from VLDL: effect of particle size. *J. Lipid Res.* **40**: 1875–1882.
47. Cohn, J. S., M. Tremblay, R. Batal, H. Jacques, C. Rodriguez, G. Steiner, O. Mamer, and J. Davignon. 2004. Increased apoC-III production is a characteristic feature of patients with hypertriglyceridemia. *Atherosclerosis.* **177**: 137–145.
48. Crawford, D. C., L. Dumitrescu, R. Goodloe, K. Brown-Gentry, J. Boston, B. McClellan, C. Sutcliffe, R. Wiseman, P. Baker, M. A. Pericak-Vance, et al. 2014. Rare variant APOC3 R19X is associated with cardio-protective profiles in a diverse population-based survey as part of the Epidemiologic Architecture for Genes Linked to Environment (EAGLE) Study. *Circ Cardiovasc Genet.* **7**: 848–853.
49. Xiao, C., and G. F. Lewis. 2012. Regulation of chylomicron production in humans. *Biochim. Biophys. Acta.* **1821**: 736–746.